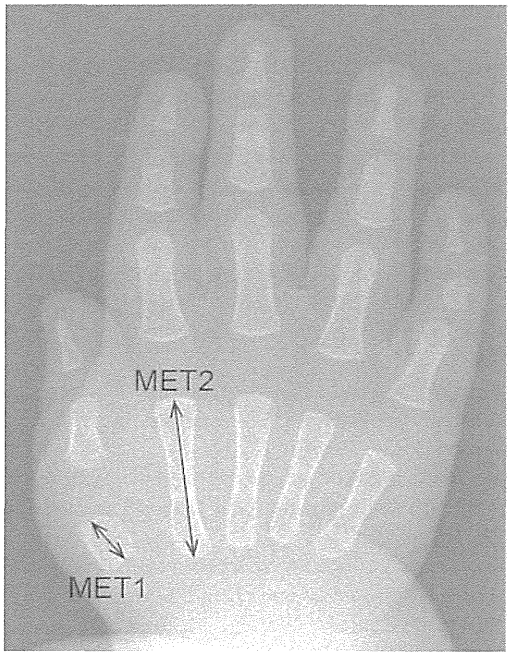

Figure 7. An anteroposterior radiograph of the right hand of Patient 1 at the age of eight months showing marked shortening of the first metacarpal bone. The MET2/MET1 ratio and the corresponding SD value is 2.9 and 16.3, respectively.

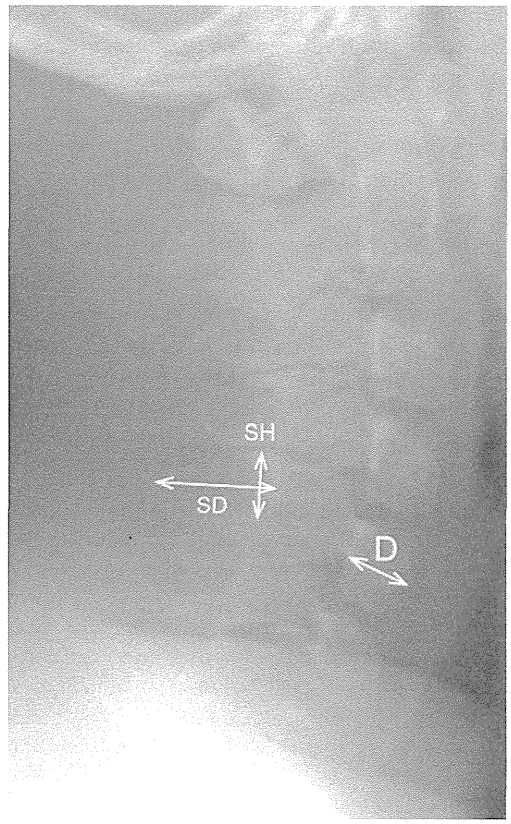

Figure 8. A lateral radiograph of the cervical spine of Patient 16 at the age of eight years showing enlarged spinous process of the C5 vertebra. The (SH+SD)/D ratio and the corresponding SD value is 2.8 and 7.9, respectively.

HoxD13 gene in the presumptive digit I area is of great significance (*13*). Mutations in the homeodomain of the *HoxD13* gene cause brachydactyly type D that is characterized by variable shortening of the distal phalanx of the thumb. This mutated HoxD13 proteins responsible for its decreased affinity for the double-stranded DNA target containing a cognitive sequence of the homeodomain (*14*). Interestingly, previous research has revealed that BMP signaling-dependent Smad1/4 proteins prevented HoxD10 and HoxD13 from binding to DNA targets (*15*). Constitutively-activated BMP signaling in FOP thus is likely to impair HoxD13-mediated transcriptional regulation by direct interactions between BMP-induced Smads and HoxD13. Mesenchymal condensation and chondrocyte proliferation of the presumptive digit I area could be suppressed by down-regulated HoxD13 function, whereas in presumptive digits II to V areas, it could be preserved by compensating expressions of other *HoxD* genes (*HoxD11* and *HoxD12*). Dysregulated BMP signal transduction during embryogenesis seems to cause relative shortening of the first metacarpals and distal phalanges of the thumb in FOP.

More than 90% of adult FOP patients showed fusion of the facet joints, which is a type of orthotopic ossification (*6*). To our knowledge, however, there are no reports delineating the precise prevalence of tall and narrow vertebral bodies and enlarged posterior elements of the cervical vertebrae. Here we demonstrated that the H/D and (SH + SD)/D ratios in the C5 vertebrae were larger than +2SD of normal values in 64% and 73% of patients, respectively (Figure 8). In addition to neck stiffness, which seemed to be an important early clinical sign before the appearance of HO (*6*), tall and narrow vertebrae and hypertrophic spinous processes of the cervical spine are radiographic characteristics in young FOP patients.

In a previous *in vivo* study, genetically-engineered overexpression of BMP-2/4 both dorsally and laterally to the neural tube manifested combined phenotypes of hypertrophic spinous processes and large deletion of the lateral and ventral parts of vertebral bodies (*16*). Thus, mesenchymal condensations at the paraxial mesoderm in FOP, where BMP-2 signaling is aberrantly activating, could be responsible for both enlarged spinous processes and relatively tall vertebral bodies.

The common *ACVR1/ALK2* mutation (c.617G > A, p.R206H) shows a homogeneous phenotype including congenital malformation of the great toes and the skeletal features in the thumb and cervical spine (*17*). In contrast, several atypical mutations in the *ALK2/ACVR1* gene, such as L196P, R258S, R375P, G328R, and P197_F198 del insL, have been identified in patients who showed normal-appearing great toes (*18*). In this study, one patient (Patient 14) with an atypical mutation (c.774G > C, p.R258S) showed normal-appearing great toes. She also lacked the shortened thumb but exhibited exceptionally tall and narrow vertebral bodies. Another patient (Patient 4) who showed neither malformed great

toes nor shortening of the first metacarpal bone also manifested distinctive features of the cervical spine in spite of the common *ACVR1/ALK2* mutation. We believe that radiographic characteristics of the cervical spine are potent diagnostic clues for FOP especially in cases without typical deformities of the great toes.

Acknowledgements

This work was supported partly by Research Committee on Fibrodysplasia Ossificans Progressiva from the Ministry of Health, Labour and Welfare of Japan.

References

1. Shore EM, Xu M, Feldman GJ, *et al.* A recurrent mutation in the BMP type I receptor ACVR1 causes inherited and sporadic fibrodysplasia ossificans progressiva. Nat Genet. 2006; 38:525-527.
2. Kitterman JA, Kantanie S, Rocke DM, Kaplan FS. Iatrogenic harm caused by diagnostic errors in fibrodysplasia ossificans progressiva. Pediatrics. 2005; 116:e654-e661.
3. Kitoh H, Achiwa M, Kaneko H, Mishima K, Matsushita M, Kadono I, Horowitz JD, Sallustio BC, Ohno K, Ishiguro N. Perhexiline maleate in the treatment of fibrodysplasia ossificans progressiva: An open-labeled clinical trial. Orphanet J Rare Dis. 2013; 8:163.
4. Pignolo RJ, Shore EM, Kaplan FS. Fibrodysplasia ossificans progressiva: Diagnosis, management, and therapeutic horizons. Pediatr Endocrinol Rev. 2013; 10 (Suppl 2):437-448.
5. Nakashima Y, Haga N, Kitoh H, Kamizono J, Tozawa K, Katagiri T, Susami T, Fukushi J, Iwamoto Y. Deformity of the great toe in fibrodysplasia ossificans progressiva. J Orthop Sci. 2010; 15:804-809.
6. Kaplan FS, Glaser DL, Shore EM, Deirmengian GK, Gupta R, Delai P, Morhart P, Smith R, Le Merrer M, Rogers JG, Connor JM, Kitterman JA. The phenotype of fibrodysplasia ossificans progressiva. Clin Rev Bone Miner Metab. 2005; 3:183-188.
7. Mishima K, Kitoh H, Katagiri T, Kaneko H, Ishiguro N. Early clinical and radiographic characteristics in fibrodysplasia ossificans progressiva: A report of two cases. J Bone Joint Surg Am. 2011; 93:e52.
8. Poznanski AK, Garn SM, Holt JF. The thumb in the congenital malformation syndromes. Radiology. 1971; 100:115-129.
9. Remes VM, Heinanen MT, Kinnunen JS, Marttinen EJ. Reference values for radiological evaluation of cervical vertebral body shape and spinal canal. Pediatr Radiol. 2000; 30:190-195.
10. Kaplan FS, Le Merrer M, Glaser DL, Pignolo RJ, Goldsby RE, Kitterman JA, Groppe J, Shore EM. Fibrodysplasia ossificans progressiva. Best Pract Res Clin Rheumatol. 2008; 22:191-205.
11. Pignolo RJ, Shore EM, Kaplan FS. Fibrodysplasia ossificans progressiva: Clinical and genetic aspects. Orphanet J Rare Dis. 2011; 6:80.
12. Oberg KC. Review of the molecular development of the thumb: Digit primera. Clin Orthop Relat Res. 2014; 472:1101-1105.
13. Deschamps J. Tailored *Hox* gene transcription and the making of the thumb. Genes Dev. 2008; 22:293-296.
14. Johnson D, Kan SH, Oldridge M, Trembath RC, Roche P, Esnouf RM, Giele H, Wilkie AO. Missense mutations in the homeodomain of HOXD13 are associated with brachydactyly types D and E. Am J Hum Genet. 2003; 72:984-997.
15. Li X, Nie S, Chang C, Qiu T, Cao X. Smads oppose Hox transcriptional activities. Exp Cell Res. 2006; 312:854-864.
16. Monsoro-Burq AH, Duprez D, Watanabe Y, Bontoux M, Vincent C, Brickell P, Le Douarin N. The role of bone morphogenetic proteins in vertebral development. Development. 1996; 122:3607-3616.
17. Kaplan FS, Xu M, Glaser DL, Collins F, Connor M, Kitterman J, Sillence D, Zackai E, Ravitsky V, Zasloff M, Ganguly A, Shore EM. Early diagnosis of fibrodysplasia ossificans progressiva. Pediatrics. 2008; 121:e1295-e1300.
18. Kaplan FS, Xu M, Seemann P, *et al.* Classic and atypical fibrodysplasia ossificans progressiva (FOP) phenotypes are caused by mutations in the bone morphogenetic protein (BMP) type I receptor ACVR1. Hum Mutat. 2009; 30:379-390.

(Received April 13, 2014; Revised April 24, 2014; Accepted May 07, 2014)

Meclozine Promotes Longitudinal Skeletal Growth in Transgenic Mice with Achondroplasia Carrying a Gain-of-Function Mutation in the *FGFR3* Gene

Masaki Matsushita[1,2], Satoru Hasegawa[1], Hiroshi Kitoh[2], Kensaku Mori[3], Bisei Ohkawara[1], Akihiro Yasoda[4], Akio Masuda[1], Naoki Ishiguro[2], Kinji Ohno[1]

1Division of Neurogenetics, Center for Neurological Diseases and Cancer, Nagoya University Graduate School of Medicine, Nagoya, Japan; [2]Department of Orthopaedic Surgery, Nagoya University Graduate School of Medicine, Nagoya, Japan; [3]Department of Media Science, Graduate School of Information Science, Nagoya University, Nagoya, Japan; [4]Department of Diabetes, Endocrinology and Nutrition, Kyoto University Graduate School of Medicine, Kyoto, Japan Key terms: meclozine, achondroplasia, FGFR3

Achondroplasia (ACH) is one of the most common skeletal dysplasias causing short stature owing to a gain-of-function mutation in the *FGFR3* gene, which encodes the fibroblast growth factor receptor 3. We found that meclozine, an over-the-counter drug for motion sickness, inhibited elevated FGFR3 signaling in chondrocytic cells. To examine the feasibility of meclozine administration in clinical settings, we investigated the effects of meclozine on ACH model mice carrying the heterozygous *Fgfr3*^{ach} transgene. We quantified the effect of meclozine in bone explant cultures employing limb rudiments isolated from developing embryonic tibiae from *Fgfr3*^{ach} mice. We found that meclozine significantly increased the full-length and cartilaginous primordia of embryonic tibiae isolated from *Fgfr3*^{ach} mice. We next analyzed the skeletal phenotypes of growing *Fgfr3*^{ach} mice and wild-type mice with or without meclozine treatment. In *Fgfr3*^{ach} mice, meclozine significantly increased the body length after two weeks of administration. At skeletal maturity, the bone lengths, including the cranium, radius, ulna, femur, tibia, and vertebrae were significantly longer in meclozine-treated *Fgfr3*^{ach} mice than in untreated *Fgfr3*^{ach} mice. Interestingly, meclozine also increased bone growth in wild-type mice. The plasma concentration of meclozine during treatment was within the range that has been used in clinical settings for motion sickness. Increased longitudinal bone growth in *Fgfr3*^{ach} mice by oral administration of meclozine in a growth period indicates potential clinical feasibility of meclozine for the improvement of short stature in ACH.

Fibroblast growth factor receptor 3 (FGFR3) is a negative regulator of endochondral bone growth. Gain-of-function mutations in the *FGFR3* gene cause several short-limbed skeletal dysplasias, including achondroplasia (ACH) (1, 2), hypochondroplasia (HCH) (3), severe ACH with developmental delay and acanthosis nigricans (SADDAN) (4), and thanatophoric dysplasia (TD) types I and II (5). In contrast, loss-of-function mutations in *FGFR3* lead to camptodactyly, tall stature, and hearing loss (CATSHL) syndrome (6). ACH is the most common short-limbed skeletal dysplasia, with an incidence of 1 in 16 000 to 26 000 live births (7). Clinical features of ACH include severe short stature with rhizomelic shortening of the extremities, relative macrocephaly with frontal bossing, midface hypoplasia, and increased lumbar lordosis. In addition, foramen magnum stenosis, hydrocephalus, and spinal canal stenosis are potentially serious complications of ACH (8).

Growth hormone has been administered to children with ACH for treatment of short stature in some countries (9), but the response to this therapy is moderate and the long-term effects remain controversial. Limb lengthening

ISSN Print 0013-7227 ISSN Online 1945-7170
Printed in U.S.A.

Received November 13, 2014. Accepted November 25, 2014.

Abbreviations:

procedures are another therapeutic option to gain bone length (10) but involves significant time and effort. Inhibition of FGFR3 signaling is a therapeutic strategy for ACH and other FGFR3-related skeletal dysplasias (11–13); however, no effective treatments are currently available for these disorders. C-type natriuretic peptide (CNP) is a potent antagonist of *FGFR3* signaling, which alleviates the short-limbed phenotype of transgenic ACH mice through inhibition of the intracellular mitogen-activated protein kinase (MAPK) pathway (14). CNP, however, has a short half-life, and continuous intravenous (IV) infusion is required for in vivo experiments (15). A CNP analog with an extended half-life, BMN-111, has recently been developed, and significant bone growth recovery was demonstrated in a mouse model of ACH by subcutaneous administration of BMN-111 (16). Recent studies using induced pluripotent stem (iPS) cells established from patients with FGFR3-related skeletal dysplasias revealed that statins also rescue the mouse phenotypes (17).

In our previous study, we found that meclozine, an overthe-counter (OTC) H1 receptor inhibitor used to treat motion sickness, inhibited elevated FGFR3 signaling and promoted chondrocyte proliferation and differentiation using various chondrocytic cell lines. We also confirmed that meclozine alleviates FGF2-mediated longitudinal growth inhibition of embryonic tibiae in bone explant cultures (18). In the present study, we orally administered meclozine to immature transgenic mice with ACH and investigated the effects of this drug on longitudinal bone growth and bone-related complications.

Materials and Methods

Mice

Fgfr3^{ach} mice (FVB background) were provided by Dr. David M. Ornitz at Washington University (19). In brief, *Fgfr3*^{ach} mice express activated *FGFR3* in the growth plate using the *Col2a1* promoter. In all experiments, we used transgenic mice carrying the heterozygous *Fgfr3*^{ach} transgene. Due to unavailability of a sufficient number of wild-type FVB mice, we employed BL6J mice to investigate the effect of meclozine on wild-type mice. All experimental procedures were approved by the Animal Care and Use Committee of our institution.

Bone explant cultures

For bone explant cultures, tibiae from *Fgfr3*^{ach} mice embryos were dissected under the microscope on embryonic day 16.5, placed in a 48-well plate, and cultured in BGJb medium (Invitrogen) supplemented with 0.2% bovine serum albumin and 150 mg/ml ascorbic acid in the presence or absence of 20 μM meclozine (MP Biomedicals). The embryonic tibiae were cultured for 6 days, with daily replenishment of the medium. The longitudinal length of the bone, which was defined as the length between the proximal and distal articular cartilage, was measured using ImageJ (18).

Oral administration of meclozine to mice

Food containing meclozine, which was prepared by mixing 0.4 g of meclozine with 1 kg of food (Oriental Yeast Co.), was administered ad libitum to (i) wild-type mice from 2 weeks of age, (ii) *Fgfr3*^{ach} and littermate mice from 3 weeks of age, or (iii) pregnant mice carrying wild-type embryos from 14 days of gestation. Body length was measured every week.

Calculation of feed intake

Fgfr3^{ach} male mice and wild-type female mice were allowed to mate and the 3-week-old littermates were divided into treated and untreated groups. Each group shared one cage for 3 weeks, and total food intake for each cage was measured. The measurements were divided by the total body weight of the mice in each cage, and the calculated values between the two groups were compared.

Radiological analysis

At the end of the treatment, *Fgfr3*^{ach} mice were subjected to microcomputed tomography (Micro-CT) scans (0.5 mm Al filter, 50 kV, 500 μA for 0.054 seconds; SkyScan 1176, Bruker) as well as a soft X-ray (30 kV, 5 mA for 20 seconds; SOFTEX Type CMB-2; SOFTEX, Kanagawa, Japan). Three-dimensional images from the CT scan were reconstructed by an in-house volume-rendering software (20). This software enabled us to render 3D views of the CT scan from arbitrary viewpoints and directions, as well as measure the distance between two specific points. The lengths of various bones, including the cranium, humerus, radius, ulna, femur, tibia, and vertebrae (L1–5) were measured on both the soft X-ray films and the reconstructed 3D images. The areas of the foramen magnum and spinal canal from L3, L4, and L5 vertebrae were measured from the reconstructed 2D images with the CT-Analyzer (Bruker). The total bone volume of each mouse was also measured from the reconstructed 3D images.

Skeletal preparation

Whole skeletons were harvested, stored in 90% ethanol for 3 days, followed by acetone treatment for 2 days (21). Specimens were then stained using Alizarin red to analyze ossified bones, and Alcian blue to analyze cartilage, for 3 days at 37°C. Following incubation, the samples were transferred to 1% KOH and incubated at room temperature for 2 days. The specimens were serially washed with decreasing concentrations (1% to 0%) of KOH and increasing concentrations (0% to 100%) of glycerol by monitoring the intensity of the stain and the amount of tissue remaining on the specimens. Longitudinal bones, including the humerus, radius, ulna, femur, and tibia were dissected under the microscope and their lengths were measured using ImageJ.

Measurement of plasma meclozine concentrations

Cardiac blood samples were collected under anesthesia from 8-week-old BL6J mice fed 0.2 g or 0.4 g meclozine per kilogram food ad libitum for 72 hours, and plasma concentrations of meclozine were measured (Tanabe R&D Service Co.).

Statistical analysis

Data are expressed as mean ± standard deviation (SD). Statistical analyses were carried out using the paired and unpaired Student's *t*-tests, or two-way ANOVA followed by Fisher's LSD test.

Results

Meclozine attenuated the growth defect in the *Fgfr3*^{ach} tibiae in bone explant culture

We quantified the effect of meclozine in bone explant cultures by using developing embryonic tibiae isolated from limb rudiments in *Fgfr3*^{ach} mice (n = 5) at embryonic day 16.5 (E16.5). We added 20 mM meclozine to the culture medium and compared the length of the treated tibia with that of the contralateral untreated tibia from the same mouse. Meclozine significantly increased the full-length and cartilaginous primordia of the tibiae from *Fgfr3*^{ach} mice by 4.6% ($P < .05$) and 8.3% ($P < .01$) as compared with the contralateral untreated tibiae, respectively. In contrast, the bone marrow in the meclozine-treated tibiae was similar to that in untreated tibiae (Figure 1).

Meclozine ameliorated the short stature of *Fgfr3*^{ach} mice

We next examined the effects of meclozine on longitudinal skeletal growth in *Fgfr3*^{ach} mice. 3-week-old littermates comprised of *Fgfr3*^{ach} and wild-type mice, which were born from *Fgfr3*^{ach} male and wild-type female, were randomly divided into two groups (a meclozine-treated group and an untreated group). Thus, a variable combination of four groups was generated for each kinship: (i) meclozine-treated *Fgfr3*^{ach} mice, (ii) meclozine-treated wild-type mice, (iii) untreated *Fgfr3*^{ach} mice, and (iv) untreated wild-type mice. *Fgfr3*^{ach} and wild-type littermates were not differentiated when meclozine treatment was started because we genotyped mice using tails at the end of the experiment in order to consecutively measure the total body length. The absolute values of the body length and bone length were compared within a kinship but not between kinships. For comparison across kinships, we used values normalized with wild-type littermates in the same kinship. We analyzed a total of 8 kinships, including 12 *Fgfr3*^{ach} mice and 19 wild-type mice. Food containing 0.4 g meclozine per kilogram was administered ad libitum to 3-week-old littermates in the treated group for 3 weeks. At six weeks, the body length of the untreated *Fgfr3*^{ach} mice was much shorter than that of the gender-matched wild-type littermates. In contrast, the body lengths of the treated *Fgfr3*^{ach} mice were closer to those of gender-matched wild-type littermates. Quantitative measurements demonstrated that meclozine increased the body length of *Fgfr3*^{ach} mice by 5.4% ($P < .05$; Figure 2A). Temporal analyses demonstrated that meclozine had a statistically significant effect on body length after two weeks (Figure 2B). Intake of food by individual mice (per one gram of the body weight) was similar between the treated and untreated groups (Supplemental Figure 1).

Meclozine increased the bone length of *Fgfr3*^{ach} mice

We next quantified the effects of meclozine on the bone growth of *Fgfr3*^{ach} mice using radiological analysis. After 3 weeks of meclozine administration, *Fgfr3*^{ach} mice were subjected to soft X-ray and Micro-CT scan. We measured individual bone lengths based on the 3D images reconstructed from the Micro-CT scan. The bone lengths, including the cranium, radius, ulna, femur, tibia, and ver-

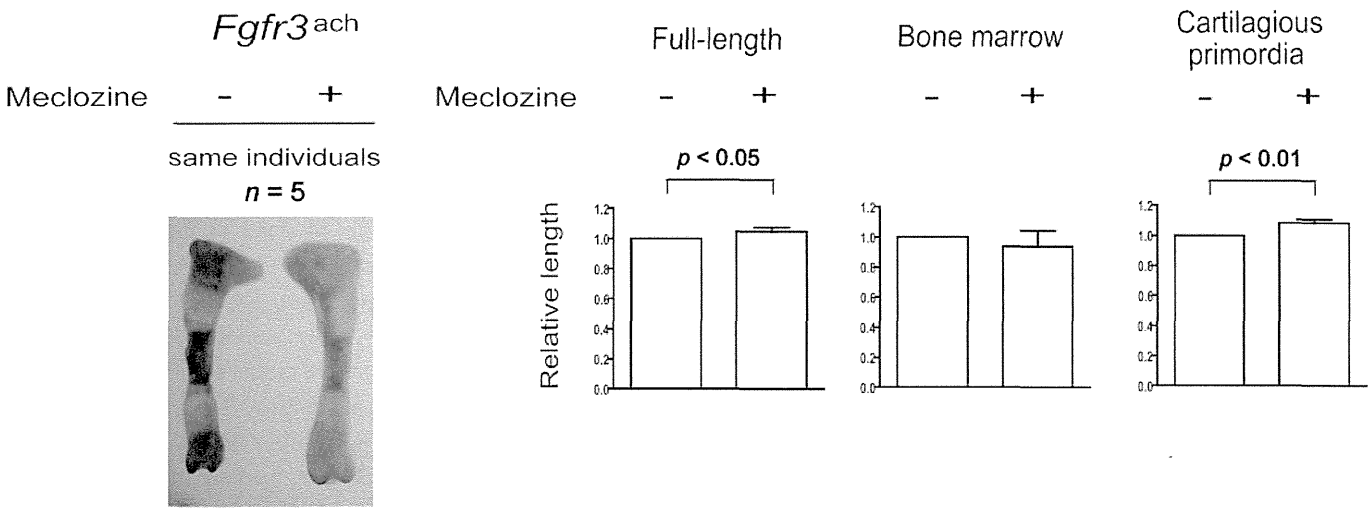

Figure 1. Meclozine enhances bone growth of embryonic tibiae in *Fgfr3*^{ach} mice in explant cultures. Meclozine significantly increased the full-length and cartilaginous primordia of tibiae in *Fgfr3*^{ach} mice but had no effect on the length of bone marrow.

tebrae (L1–5) were significantly longer in meclozine-treated $Fgfr3^{ach}$ mice than in the untreated $Fgfr3^{ach}$ mice (Figure 3A). Similar results were obtained from measurements using the soft X-ray films (Supplemental Figure 2). The bone volumes of the $Fgfr3^{ach}$ mice, measured from osseous voxels on the reconstructed images, were significantly increased by meclozine treatment (Figure 3B).

We further analyzed the area of the foramen magnum and lumbar spinal canal in $Fgfr3^{ach}$ mice. Meclozine did not increase the area of foramen magnum and lumbar spinal canal in $Fgfr3^{ach}$ mice (Supplemental Figure 3 and 4).

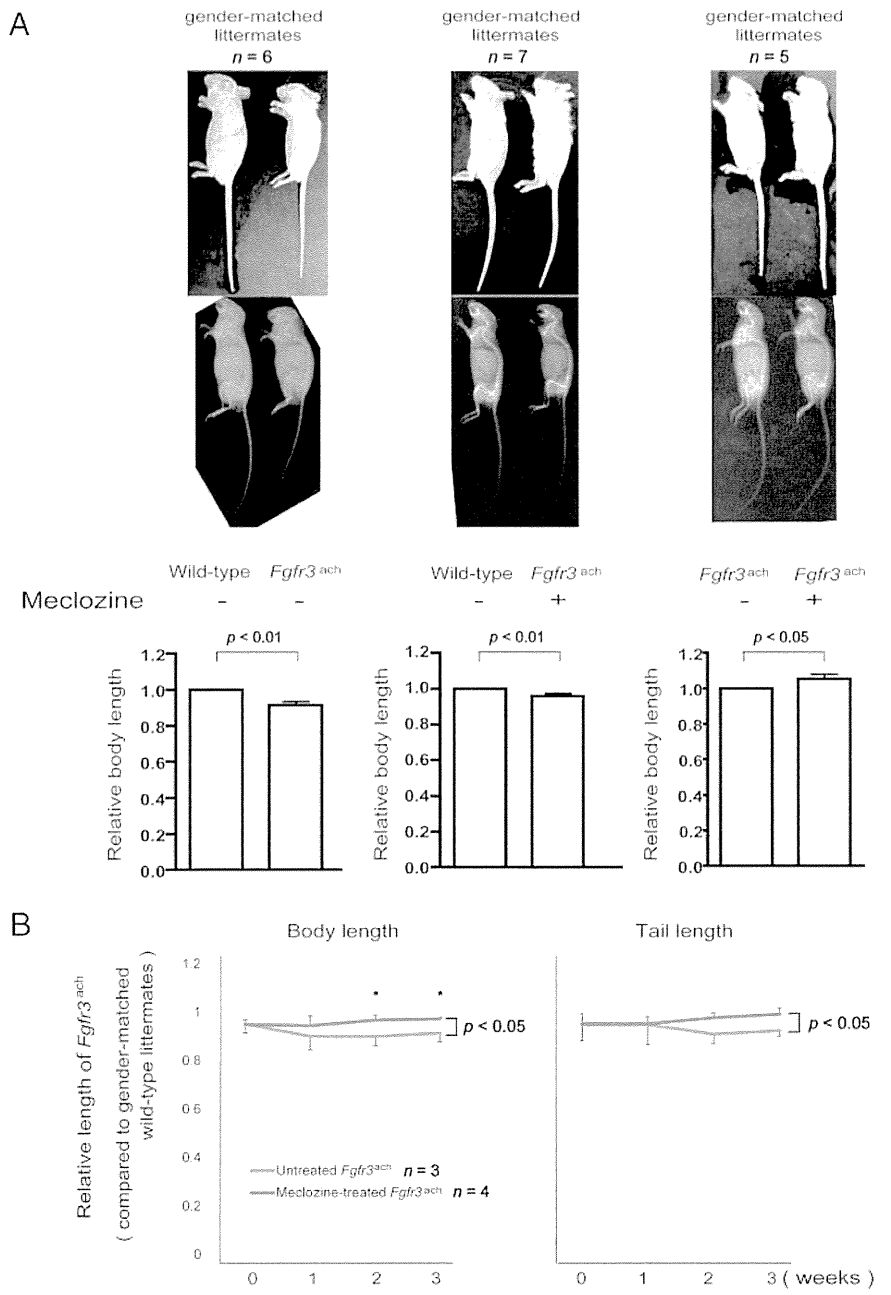

Figure 2. Meclozine reverses the dwarfed phenotype in $Fgfr3^{ach}$ mice. A, Meclozine treatment was initiated without prior knowledge of the genotype and administered for 3 weeks. 3 indicated pairs of gender-matched littermates were examined. Body length of the mice was normalized to that of the indicated gender-matched wild-type littermate. Body lengths of $Fgfr3^{ach}$ mice without meclozine treatment were 0.913 ± 0.023 of the gender-matched wild-type littermates (left graph). The body lengths of $Fgfr3^{ach}$ mice with meclozine treatment were 0.960 ± 0.018 of the gender-matched wild-type littermates (middle graph). Meclozine significantly increased the body length of $Fgfr3^{ach}$ mice ($P < .05$ by unpaired t test, not shown). In 5 kinships, in which gender-matched $Fgfr3^{ach}$ mice were treated with or without meclozine, meclozine increased the body length of $Fgfr3^{ach}$ mice to 1.054 ± 0.027 of the untreated $Fgfr3^{ach}$ mice (right graph). Left panel, a male pair; middle panel, a female pair and right panel, a male pair. Mean and standard deviation (SD) are indicated in the graphs and the legends. The statistical differences shown on each graph were analyzed by paired t test. B, The body and tail lengths of meclozine-treated $Fgfr3^{ach}$ mice were significantly longer than those of untreated $Fgfr3^{ach}$ mice. The measured lengths of the $Fgfr3^{ach}$ mice were normalized to those of the gender-matched wild-type littermates. Statistical significance by two-way ANOVA is shown on the right side of each graph. $*P < .05$ by Fisher's LSD test for each pair.

Meclozine increased the bone growth in wild-type mice

We further examined the effects of meclozine on bone growth in wild-type mice. Meclozine was administrated to 2-week-old wild-type mice for 3 weeks. As wild-type mice were weaned at 2 weeks after birth, we started meclozine treatment 1 week earlier than that for $Fgfr3^{ach}$ mice. The body length of meclozine-treated mice was significantly longer than that of untreated mice after 1 week (Figure 4A, B). The bone lengths of the radius, ulna, femur, tibia, and vertebrae (L1–5) of the meclozine-treated mice were significantly longer than the corresponding bone lengths in the untreated mice (Figure 4C).

We next administered meclozine to pregnant wild-type mice to examine the effects of the drug on fetal bone development. After administration of meclozine to wild-type mice at 14 days of gestation, their offspring were subjected to transparent specimen analysis at postnatal day 5. The meclozine-treated offspring were larger than the untreated offspring (Figure 4D). The lengths of the long tubular bones, including the ulna, femur, and tibia, were significantly longer in the meclozine-

treated mice than in the untreated-mice (Figure 4E).

The plasma meclozine concentration in the present study is clinically relevant

We next measured the plasma concentrations of meclozine used in the current study (0.2 or 0.4 g of meclozine per kilogram food). Blood samples were collected from 8-week-old wild-type mice after ad libitum intake of meclozine-containing food for 72 hours. The average plasma meclozine concentrations after treatment were within the range used in clinical settings (22) (Figure 5).

Discussion

The small compounds, NF449 (11), A31 (12), and P3 (13), have recently been reported to improve short-stature phenotypes in animal models with accelerated FGFR3 signaling. The safety of these novel compounds in humans, however, remains to be elucidated. Meclozine, an OTC H1 inhibitor, has been safely used for motion sickness for more than 50 years, and its optimal dose and adverse effects have already been established. A previous study indicates that the peak plasma concentration of meclozine is 68.42 ng/ml after a single clinical dose in humans (22). We have demonstrated that oral administration of clinically attainable concentrations of meclozine increased longitudinal bone growth in *Fgfr3*^{ach} mice during the observed growth period. This effect was most likely due to the inhibition of activated FGFR3 signaling, which was previously observed in cultured rat chondrosarcoma cells (18). Currently, distraction osteogenesis is the only available surgical procedures to increase bone length; however, it is a long and invasive treatment that compromises the patient's quality of life (QOL). The healing index is 36.2 days per cm (23); thus, the patients are forced to attach external fixators for 362 days to increase their height by 10 cm. In contrast, meclozine increased body length of *Fgfr3*^{ach} mice by 5.4% in our study. If the same effect could be observed in patients with ACH, the patients could be expected to increase 6.7 to 7.1 cm in height, based on the average height of adults with ACH. Although further studies are needed to investigate the adverse effects associated with long-term drug administration, meclozine is a potential therapeutic compound for ACH and other FGFR3-related disorders.

To date, CNP, the CNP analog BNM-111, and statins are the only promising compounds that can be applied in clinical practice for FGFR3-related skeletal disorders. Yasoda et al reported that continuous IV administration of CNP rescued the short-limbed phenotype in *Fgfr3*^{ach} mice (15). Lorget et al similarly demonstrated that subcutaneous injection of BNM-111 reversed the dwarfism-related clinical features observed in *Fgfr3*$^{Y367C/+}$ mice (16). Additionally, Yamashita et al identified that intraperitoneal injection of statins, which have been used to lower serum cholesterol levels, rescued the phenotype of *Fgfr3*^{ach} mice using a screen with patient-derived iPS cells (17). Currently, CNP and BNM-111 administration is restricted to injection, which potentially poses physical and psychological burdens on young children. Since meclozine and statins can be administered orally, they are more convenient for children to take. Although the site of action of statins has not been dissected (17), meclozine and statins may have an additive effect on abnormally activated FGFR3 signaling in patients with ACH.

Some ACH patients have neurological complications such as gait disturbance, leg paralysis, hydrocephalus, and

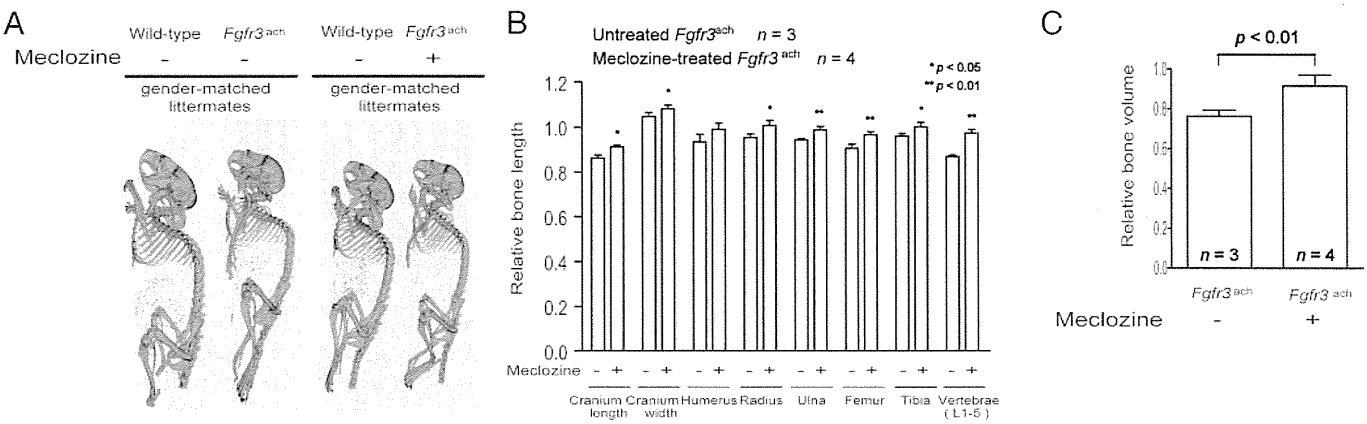

Figure 3. Meclozine increases the longitudinal bone growth of *Fgfr3*^{ach} mice. A, Reconstructed computed tomography (CT) images. Left panel, a male pair; right panel, a female pair. B, Meclozine significantly increased the length of the cranium, radius, ulna, femur, tibia, and vertebrae in *Fgfr3*^{ach} mice. C, The total bone volume of meclozine-treated *Fgfr3*^{ach} mice was significantly increased compared to that of untreated *Fgfr3*^{ach} mice. B and C, Bone lengths and total bone volumes of *Fgfr3*^{ach} mice were normalized to those of the gender-matched wild-type littermates. Statistical significance was analyzed by the unpaired *t* test.

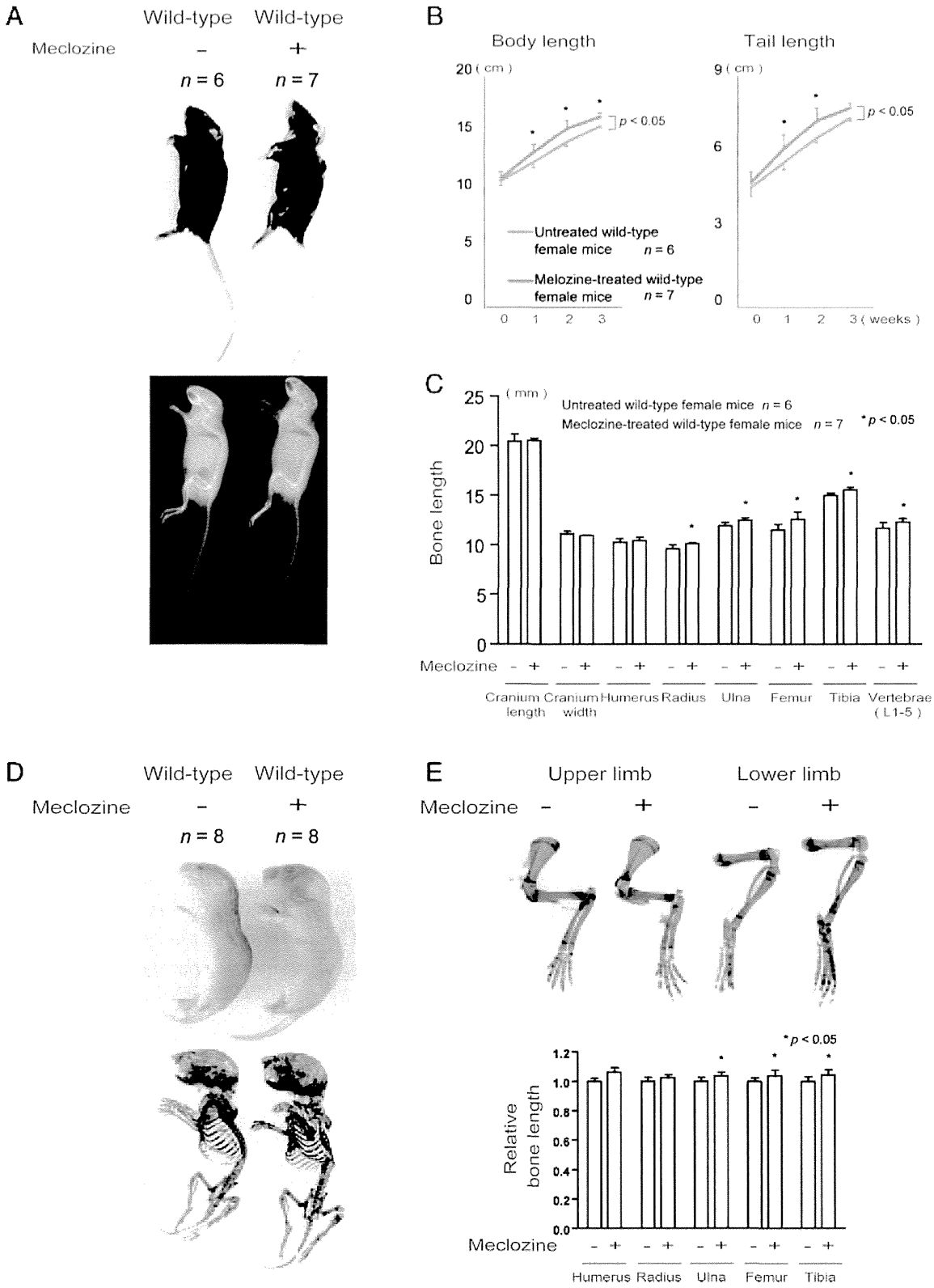

Figure 4. A-C, Wild-type mice were treated with meclozine 2 weeks after birth for 3 weeks. A, Visual images and soft X-ray images of wild-type female mice with or without meclozine. Meclozine-treated mice were larger than the untreated mice. B, Body and tail lengths of meclozine-treated wild-type female mice were significantly longer than those of untreated wild-type female mice. Statistical significance analyzed by two-way ANOVA is shown on the right side of each graph. *$P < .05$ by Fisher's LSD test for each pair. C, The lengths of the radius, ulna, femur, tibia, and vertebrae on the soft X-ray films were significantly increased by meclozine treatment by unpaired *t* test. D and E, Pregnant mice were treated with meclozine from embryonic day 14. D, Visual images and skeletons stained with Alizarin red and Alcian blue of wild-type mice at postnatal day 5, with or without meclozine. Meclozine-treated offspring were larger than untreated offspring. E, The lengths of the ulna, femur, and tibia measured using stained skeletons were significantly increased after meclozine treatment, as assessed by unpaired *t* test.

central hypopnea, in addition to short stature, which is caused by stenosis of the foramen magnum or spinal canal. In the current study, meclozine failed to enhance the growth of the foramen magnum and lumbar spinal canal. Similarly, BMN-111 could not increase the sagittal and lateral diameters of the foramen magnum in *Fgfr3*$^{Y367C/+}$ mice (16). Stenosis of the spinal canal and foramen magnum in patients with ACH is most likely due to premature synchondrosis closure, and any growth-promoting treatment for these stenoses must precede the timing of the synchondrosis closure (24). Jin et al demonstrated that the thanatophoric phenotypes of *Fgfr3*$^{K644E/+}$ mice were rescued by intraperitoneal injection of P3 to the mother (13). Prenatal treatments are generally unrealistic even if the patients get a definite diagnosis of ACH during prenatal periods. Therefore, we tested the effect of meclozine from 3 weeks of age in *Fgfr3*^{ach} mice. In future, we will examine the effect of maternal administration of meclozine using mouse models to treat devastating phenotypes in thanatophoric dysplasia and possibly stenosis of the spinal canal and foramen magnum in ACH.

Acknowledgments

We would like to thank Dr. David M. Ornitz at Washington University for providing *Fgfr3*^{ach} mice. This work was supported by Grants-in-Aid from the Ministry of Education, Culture, Sports, Science, and Technology of Japan, and the Ministry of Health, Labor, and Welfare of Japan.

Address all correspondence and requests for reprints to: Kinji Ohno, MD, PhD, 65 Tsurumai, Showa-ku, Nagoya 466–8550, Japan, Email: ohnok@med.nagoya-u.ac.jp, Phone: +81 52 744 2447, Fax: +81 52 744 2449

Disclosure Summary: The authors have nothing to disclose

This work was supported by ***Funding***: This work was supported by Grants-in-Aid from the Ministry of Education, Culture, Sports, Science, and Technology of Japan, and the Ministry of Health, Labor and Welfare of Japan.

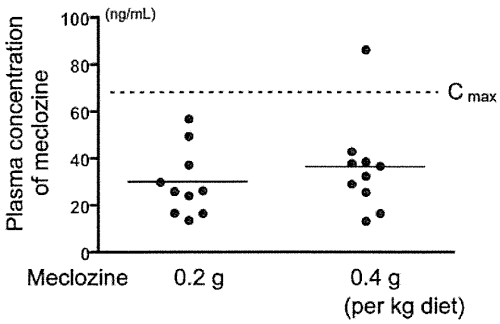

Figure 5. Plasma concentrations of meclozine in 8-week-old wild-type mice fed 0.2 g or 0.4 g meclozine per kilogram diet for 72 hours. The average plasma concentrations were 30.30 ± 14.27 ng/ml and 36.58 ± 20.12 ng/ml for 0.2 g and 0.4 g per kilogram diet, respectively. The mean peak drug concentration (C_{max}) after a single dose of 25 mg of meclozine in human subjects was 68.42 ng/ml (22).

References

1. **Rousseau F, Bonaventure J, Legeai-Mallet L, Pelet A, Rozet JM, Maroteaux P, Le Merrer M, Munnich A.** Mutations in the gene encoding fibroblast growth factor receptor-3 in achondroplasia. *Nature.* 1994;371:252–254.
2. **Shiang R, Thompson LM, Zhu YZ, Church DM, Fielder TJ, Bocian M, Winokur ST, Wasmuth JJ.** Mutations in the transmembrane domain of FGFR3 cause the most common genetic form of dwarfism, achondroplasia. *Cell.* 1994;78:335–342.
3. **Prinos P, Costa T, Sommer A, Kilpatrick MW, Tsipouras P.** A common FGFR3 gene mutation in hypochondroplasia. *Hum Mol Genet.* 1995;4:2097–2101.
4. **Tavormina PL, Bellus GA, Webster MK, Bamshad MJ, Fraley AE, McIntosh I, Szabo J, Jiang W, Jabs EW, Wilcox WR, Wasmuth JJ, Donoghue DJ, Thompson LM, Francomano CA.** A novel skeletal dysplasia with developmental delay and acanthosis nigricans is caused by a Lys650Met mutation in the fibroblast growth factor receptor 3 gene. *Am J Hum Genet.* 1999;64:722–731.
5. **Tavormina PL, Shiang R, Thompson LM, Zhu YZ, Wilkin DJ, Lachman RS, Wilcox WR, Rimoin DL, Cohn DH, Wasmuth JJ.** Thanatophoric dysplasia (types I and II) caused by distinct mutations in fibroblast growth factor receptor 3. *Nat Genet.* 1995;9:321–328.
6. **Toydemir RM, Brassington AE, Bayrak-Toydemir P, Krakowiak PA, Jorde LB, Whitby FG, Longo N, Viskochil DH, Carey JC, Bamshad MJ.** A novel mutation in FGFR3 causes camptodactyly, tall stature, and hearing loss (CATSHL) syndrome. *Am J Hum Genet.* 2006;79:935–941.
7. **Waller DK, Correa A, Vo TM, Wang Y, Hobbs C, Langlois PH, Pearson K, Romitti PA, Shaw GM, Hecht JT.** The population-based prevalence of achondroplasia and thanatophoric dysplasia in selected regions of the US. *Am J Med Genet A.* 2008;146A:2385–2389.
8. **Horton WA, Hall JG, Hecht JT.** *Achondroplasia. Lancet.* 2007;370:162–172.
9. **Horton WA, Hecht JT, Hood OJ, Marshall RN, Moore WV, Hollowell JG.** Growth hormone therapy in achondroplasia. *Am J Med Genet.* 1992;42:667–670.
10. **Noonan KJ, Leyes M, Forriol F, Canadell J.** Distraction osteogenesis of the lower extremity with use of monolateral external fixation. A study of two hundred and sixty-one femora and tibiae. *J Bone Joint Surg Am.* 1998;80:793–806.
11. **Krejci P, Murakami S, Prochazkova J, Trantirek L, Chlebova K, Ouyang Z, Aklian A, Smutny J, Bryja V, Kozubik A, Wilcox WR.** NF449 is a novel inhibitor of fibroblast growth factor receptor 3 (FGFR3) signaling active in chondrocytes and multiple myeloma cells. *J Biol Chem.* 2010;285:20644–20653.
12. **Jonquoy A, Mugniery E, Benoist-Lasselin C, Kaci N, Le Corre L, Barbault F, Girard AL, Le Merrer Y, Busca P, Schibler L, Munnich A, Legeai-Mallet L.** A novel tyrosine kinase inhibitor restores chondrocyte differentiation and promotes bone growth in a gain-of-function Fgfr3 mouse model. *Hum Mol Genet.* 2012;21:841–851.
13. **Jin M, Yu Y, Qi H, Xie Y, Su N, Wang X, Tan Q, Luo F, Zhu Y, Wang Q, Du X, Xian CJ, Liu P, Huang H, Shen Y, Deng CX, Chen D, Chen L.** A novel FGFR3-binding peptide inhibits FGFR3 signaling and reverses the lethal phenotype of mice mimicking human thanatophoric dysplasia. *Hum Mol Genet.* 2012;21:5443–5455.
14. **Yasoda A, Komatsu Y, Chusho H, Miyazawa T, Ozasa A, Miura M, Kurihara T, Rogi T, Tanaka S, Suda M, Tamura N, Ogawa Y, Nakao K.** Overexpression of CNP in chondrocytes rescues achon-

droplasia through a MAPK-dependent pathway. *Nat Med.* 2004; 10:80–86.
15. **Yasoda A, Kitamura H, Fujii T, Kondo E, Murao N, Miura M, Kanamoto N, Komatsu Y, Arai H, Nakao K.** Systemic administration of C-type natriuretic peptide as a novel therapeutic strategy for skeletal dysplasias. *Endocrinology.* 2009;150:3138–3144.
16. **Lorget F, Kaci N, Peng J, Benoist-Lasselin C, Mugniery E, Oppeneer T, Wendt DJ, Bell SM, Bullens S, Bunting S, Tsuruda LS, O'Neill CA, Di Rocco F, Munnich A, Legeai-Mallet L.** Evaluation of the therapeutic potential of a CNP analog in a Fgfr3 mouse model recapitulating achondroplasia. *Am J Hum Genet.* 2012;91:1108–1114.
17. **Yamashita A, Morioka M, Kishi H, Kimura T, Yahara Y, Okada M, Fujita K, Sawai H, Ikegawa S, Tsumaki N.** Statin treatment rescues FGFR3 skeletal dysplasia phenotypes. *Nature.* 2014;513:507–511.
18. **Matsushita M, Kitoh H, Ohkawara B, Mishima K, Kaneko H, Ito M, Masuda A, Ishiguro N, Ohno K.** Meclozine facilitates proliferation and differentiation of chondrocytes by attenuating abnormally activated FGFR3 signaling in achondroplasia. *PLoS One.* 2013;8: e81569.
19. **Naski MC, Colvin JS, Coffin JD, Ornitz DM.** Repression of hedgehog signaling and BMP4 expression in growth plate cartilage by fibroblast growth factor receptor 3. *Development.* 1998;125:4977–4988.
20. **Mori K, Suenaga Y, Toriwaki J.** Fast software-based volume rendering using multimedia instructions on PC platforms and its application to virtual endoscopy. *Proc SPIE.* 2003;5031:111–122.
21. **Wallin J, Wilting J, Koseki H, Fritsch R, Christ B, Balling R.** The role of Pax-1 in axial skeleton development. *Development.* 1994;120: 1109–1121.
22. **Wang Z, Lee B, Pearce D, Qian S, Wang Y, Zhang Q, Chow MS.** Meclizine metabolism and pharmacokinetics: formulation on its absorption. *J Clin Pharmacol.* 2012;52:1343–1349.
23. **Kitoh H, Kitakoji T, Tsuchiya H, Katoh M, Ishiguro N.** Distraction osteogenesis of the lower extremity in patients with achondroplasia/hypochondroplasia treated with transplantation of culture-expanded bone marrow cells and platelet-rich plasma. *Journal of pediatric orthopedics.* 2007;27:629–634.
24. **Matsushita T, Wilcox WR, Chan YY, Kawanami A, Bukulmez H, Balmes G, Krejci P, Mekikian PB, Otani K, Yamaura I, Warman ML, Givol D, Murakami S.** FGFR3 promotes synchondrosis closure and fusion of ossification centers through the MAPK pathway. *Hum Mol Genet.* 2009;18:227–240.

Nationwide radiation dose survey of computed tomography for fetal skeletal dysplasias

Osamu Miyazaki, Hideaki Sawai, Jun Murotsuki, Gen Nishimura & Tetsuya Horiuchi

Pediatric Radiology

ISSN 0301-0449

Pediatr Radiol
DOI 10.1007/s00247-014-2916-1

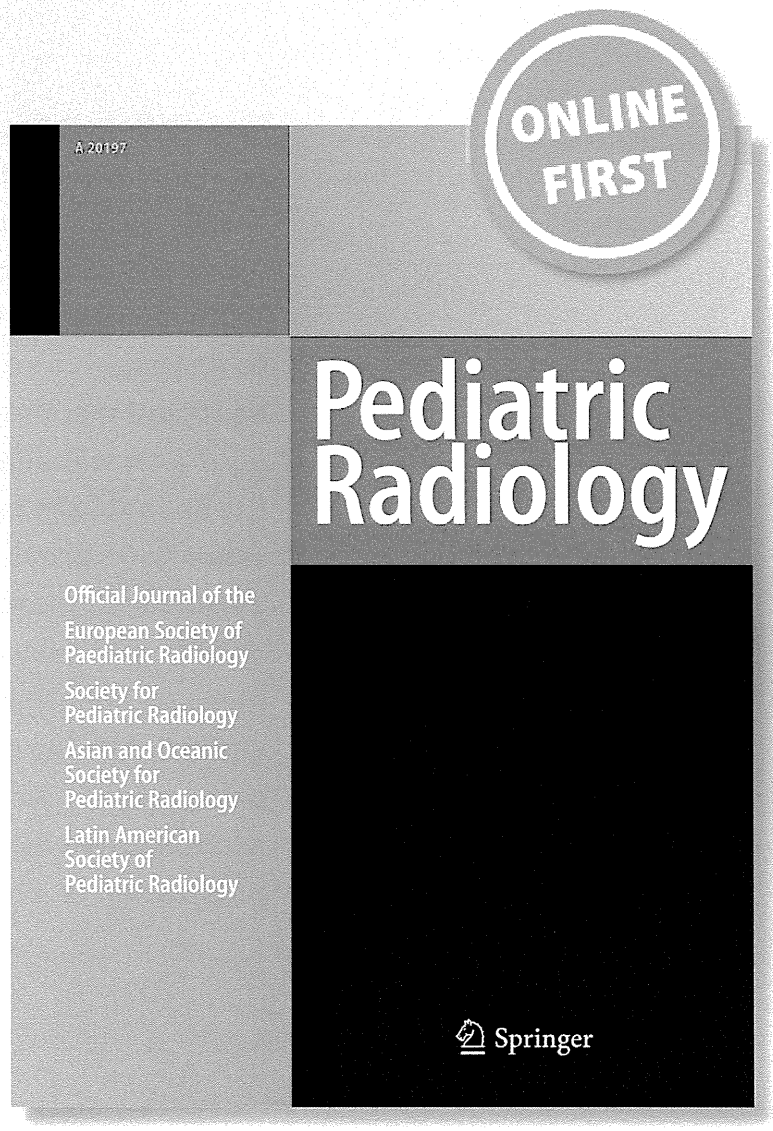

Springer

Pediatr Radiol
DOI 10.1007/s00247-014-2916-1

ORIGINAL ARTICLE

Nationwide radiation dose survey of computed tomography for fetal skeletal dysplasias

Osamu Miyazaki · Hideaki Sawai · Jun Murotsuki · Gen Nishimura · Tetsuya Horiuchi

Received: 13 June 2013 / Revised: 20 November 2013 / Accepted: 30 January 2014

Abstract
Background Recently, computed tomography (CT) has been used to diagnose fetal skeletal dysplasia. However, no surveys have been conducted to determine the radiation exposure dose and the diagnostic reference level (DRL).
Objective To collect CT dose index volume (CTDIvol) and dose length product (DLP) data from domestic hospitals implementing fetal skeletal 3-D CT and to establish DRLs for Japan.
Materials and methods Scan data of 125 cases of 20 protocols from 16 hospitals were analyzed. The minimum, first-quartile, median, third-quartile and maximum values of CTDIvol and DLP were determined. The time-dependent change in radiation dose setting in hospitals with three or more cases with scans was also examined.
Results The minimum, first-quartile, median, third-quartile and maximum CTDIvol values were 2.1, 3.7, 7.7, 11.3 and 23.1 mGy, respectively, and these values for DLP were 69.0, 122.3, 276.8, 382.6 and 1025.6 mGy·cm, respectively. Six of the 12 institutions reduced the dose setting during the implementation period.
Conclusions The DRLs of CTDIvol and DLP for fetal CT were 11.3 mGy and 382.6 mGy·cm, respectively. Institutions implementing fetal CT should use these established DRLs as the standard and make an effort to reduce radiation exposure by voluntarily decreasing the dose.

Keywords Skeletal dysplasia · Prenatal diagnosis · 3-D computed tomography · Diagnostic reference level · Fetus · Fetal computed tomography

O. Miyazaki (✉) · T. Horiuchi
Department of Radiology,
National Center for Child Health and Development,
2-10-1 Okura, Setagaya-ku, Tokyo 157-8535, Japan
e-mail: osamu-m@rc4.so-net.ne.jp

H. Sawai
Department of Obstetrics and Gynecology,
Hyogo College of Medicine,
1-1 Mukogawa-cho, Nishinomiya-shi, Hyogo 663-8501, Japan

J. Murotsuki
Department of Maternal and Fetal Medicine,
Miyagi Children's Hospital,
4-3-17 Ochiai, Aoba-ku, Sendai-shi, Miyagi 989-3126, Japan

J. Murotsuki
Department of Advanced Fetal and Developmental Medicine,
Tohoku University Graduate School of Medicine, 1-1 Seiryo-cho,
Sendai-shi, Miyagi 980-8574, Japan

G. Nishimura
Department of Pediatric Imaging,
Tokyo Metropolitan Children's Medical Center,
2-8-29 Musashidai, Fuchu-shi, Tokyo 183-8525, Japan

T. Horiuchi
Department of Medical Physics and Engineering,
Division of Medical Technology and Science,
Course of Health Science, Graduate School of Medicine,
Osaka University, 1-7 Yamadaoka, Suita, Osaka 565-0871, Japan

Introduction

In recent years, improvements in computed tomography (CT) performance have created various innovative scan techniques and increased the number of indications, such as cardiac CT. One of the new diagnostic methods is to apply CT for the prenatal diagnosis of skeletal dysplasia suspected in a fetus.

According to the latest nosology and classification of genetic skeletal disorders in 2011 [1], 456 skeletal dysplasias have been identified. The overall prevalence of neonatally manifested skeletal dysplasia is approximately 2 out of 10,000, half of them lethal [2]. However, most of these types are so rare that obstetricians never encounter them. These types include various severe diseases, from poor-prognosis diseases causing fetal or postpartum death to favorable-prognosis diseases causing no problems in physiology or intelligence.

Published online: 16 April 2014

Two-dimensional ultrasonography (2-D US) [3] and magnetic resonance imaging (MRI) [4] are conventionally used for evaluating fetal skeletal dysplasia. However, US and MRI have limitations in visualizing the skeletal system compared to radiography, which is better for performing bone surveys. Three-dimensional US [5], which was recently introduced in daily practice, provides higher image quality, but it is highly dependent on the skills of the operator. In particular, when interpreting skeletal findings in patients, the operator must create 3-D images using his/her own judgment based on his/her experience and knowledge of radiological findings. Therefore, prenatal diagnosis of skeletal dysplasia is difficult, and patients, their families and medical practitioners face difficult problems when making decisions regarding antenatal care and delivery.

Recently, fetal CT using a multidetector technique has gained popularity in the prenatal diagnosis of severe skeletal dysplasias [3, 6–11]. A precise diagnosis of skeletal dysplasia requires identification of pathognomonic findings in a constellation of as many abnormal skeletal changes as possible. Pathognomonic findings may be divided into gross changes and important, but subtle, changes. The capability of fetal CT to delineate the fetal skeleton is similar to that of a postnatal full skeletal survey. Fetal US and MRI are only able to detect gross pathognomonic changes, such as shortness, bending and deformity of the long bones, and severe skull deformity [10]. Fetal CT has been found to be highly effective in diagnosing fetal skeletal dysplasia with a diagnostic yield of 90% or higher [7, 10].

The time of 26–30 gestational weeks is recommended for the timing of fetal CT in this scenario because fetal skeletal mineralization is usually sufficient for evaluation by CT at this time [12]. Additionally, the risk of the central nervous system is greatest with exposure at 8–15 weeks of gestation, with no proven risk at greater than 25 weeks of gestation [13].

Despite this benefit, the resulting radiation exposure is disadvantageous. Whether fetal CT can be justified under the ALARA (As Low As Reasonably Achievable) principle of protection against radiation remains controversial [14]. The fetal CT technique should be more strongly justified and optimized than any other X-ray examination on the basis of the linear non-threshold hypothesis that the risk of future carcinogenesis from fetal exposure cannot be completely ruled out [15].

Bach-Segura [16] introduced adequate scan settings for fetal CT and they described an average volume CT dose index (CTDIvol) of 6 mGy at 100 kV and 120 mAs. To date, there is no guideline for fetal CT in Japan and individual hospitals may perform fetal CT according to their own protocol. If radiologists and obstetricians affirm and continue this type of examination, a guideline for fetal CT, including indications and standard protocol, should be established in the near future. In such cases, the concept of diagnostic reference levels (DRLs) is essential.

DRL is a practical tool for promoting the assessment of existing protocols and appropriate development of new and improved protocols at each CT center by facilitating the comparison of doses from present practice. DRLs were first successfully implemented in relation to conventional X-rays in the 1980s and subsequently developed for application to CT in the 1990s [17, 18]. DRLs assist in the optimization of protection by helping to avoid unnecessarily high doses to the patient. The system for using DRLs includes the estimation of patient doses as part of the regular quality assurance program [19].

DRLs are established on the basis of a survey of the standard diagnostic radiation dose that is commonly used. Each hospital can use the established DRL to optimize the diagnostic radiation dose, confirming that the dose is not much different from the DRL. The setting of DRLs and the validation of their compatibility with the clinical dose involve various factors, including the country, region, clinical purpose, guarantee of image quality, optimization of scan settings, scanner design and maintenance. However, each institution should adjust its standard radiation dose if the dose differs from the DRL without a justifiable reason.

DRLs are based on standard phantom or patient measurements under specific conditions at a number of representative clinical facilities. DRLs have been set at approximately the 75th percentile of measured patient or phantom data. This means that procedures performed at 75% of the institutions surveyed have exposure levels at or below the DRL [20]. Twenty-five percent of recorded doses will be above this level. Institutions should receive feedback on their dose levels with respect to the DRLs [21]. Few surveys or studies on fetal CT doses have been conducted [10, 22], and the fetal CT radiation dose distribution throughout Japan is unknown.

The objective of this study was to collect data on CTDIvol and dose-length product (DLP) from domestic hospitals implementing fetal 3-D CT, evaluate their trends and establish DRLs in Japan on the basis of the survey results. The Ministry of Health, Labour and Welfare of Japan (MHLW) H23-Nanchi-Ippan-123 fetal skeletal dysplasia study group takes responsibility for feeding back information to participating institutions regarding local dose levels with respect to DRLs.

Materials and methods

Data collection

We selected hospitals participating in the Japan Forum of Fetal Skeletal Dysplasia (the nation's largest online network intended to support the diagnosis of fetal skeletal dysplasia including mainly obstetricians [53 registrants]) that had already implemented fetal CT. We also selected hospitals that had consulted the Japan Forum of Fetal Skeletal Dysplasia

about fetal CT diagnosis in the past, hospitals that had reported implementation of fetal CT in abstracts issued by Japanese academic societies and scientific meetings, and the members of the MHLW Fetal Skeletal Dysplasia Study Group (grant-in-aid for Scientific Research from the Ministry of Health, Labor and Welfare of Japan H23-Nanchi-Ippan-123). A questionnaire was distributed electronically by e-mail for radiologists or obstetricians.

Thirty-eight hospitals were requested to participate in our study, and 16 of them expressed their intention to do so. These comprised eight university hospitals (Hokkaido University Hospital, Tohoku University Hospital, Yamagata University Hospital, National Defense Medical College Hospital, Hyogo College of Medicine Hospital, Tokushima University Hospital, Hiroshima University Hospital and Kurume University Hospital), five perinatal medical centers or pediatric hospitals (Miyagi Children's Hospital, National Center for Child Health and Development, Nagara Medical Center, Ehime Prefectural Central Hospital, and Perinatal Medical Center for Mother and Child Health, and Yamaguchi Grand Medical Center), and three regional referral hospitals (Aomori Prefectural Central Hospital, Chiba Kaihin Municipal Hospital and Kumamoto City Hospital). All fetuses were suspected of having skeletal dysplasias on the basis of a 2-D US scan or a second- or third-level diagnostic 2-D US performed by experienced fetal medicine physicians. After informed consent, the mothers underwent multidetector CT (mean ± SD: 30.2±2.6 weeks of gestation, range: 15–38 weeks, Table 1).

The first half of the distributed questionnaire was associated with epidemiological background, the number of fetal CT scans performed throughout the time span of the study, the timing of gestational week at multidetector CT, experience of a repeat fetal CT scan and control of fetal motion to avoid rescanning. The second half contained detailed questions on the scan conditions, including the specific CT scanner model, tube voltage (kVp), scan field of view, rotation time, number of detector rows, beam width and pitch factor. For Toshiba users, filters and parameters for volume exposure control, such as target standard deviation (SD), slice thickness, reconstruction function, and maximum and minimum tube current (mA), were asked. For GE scanners, parameters for auto mA/smart mA (type of automatic exposure control, noise index, and maximum and minimum mA) were asked. For Siemens scanners, parameters for CARE Dose 4D (quality reference mAs, and minimum and maximum of effective mAs) were asked. For the dose information, CTDIvol and DLP were collected. One hospital (hospital 8 in Table 1) changed its protocols three times during the period. Two hospitals (hospitals 4 and 13 in Table 1) used two different CT scanners, each with its own scan setting. Therefore, these situations were treated as separate protocols in this survey.

The data were entered manually into an Excel spreadsheet (Microsoft Corp., Redmond, WA, USA) by individual CT technologists in each institution, and some data were missing or inadequate in some answers. If the CTDIvol and DLP values were inappropriate, they were calculated as well as

Table 1 Results of the epidemiological background (hospital number and characteristic, number of fetal CT scans performed throughout the time span of the study, timing of gestational week at MDCT, experience of repeat fetal CT scan and fetal motion control to avoid rescanning)

Hospital	Characteristic	Fetal CT cases/years	Gestational week at MDCT (range, mean)	Experience of repeat fetal CT examination	Fetal motion control to avoid rescan
1	University hospital	7/4	25–36, 31	No	No
2	Regional referral hospital	4/3	30–34, 32	No	No
3	Perinatal medical center	4/2	20–34, 29	No	No
4	University hospital	18/6	27–36, 32	No	Mioblock
5	University hospital	5/5	27–35, 31	No	No
6	University hospital	4/5	25–28, 26	No	No
7	Regional referral hospital	2/3	15–33, 24	No	No
8	Perinatal medical center	53/5	15–37, 30	No	No
9	Perinatal medical center	11/3	26–31, 29	1 case	No
10	University hospital	4/3	28–32, 30	No	No
11	University hospital	3/3	28–30, NA	No	No
12	Perinatal medical center	4/3	29–38, 32	No	No
13	University hospital	13/6	20–35, 29	No	No
14	Perinatal medical center	3/4	28–32, 30	No	No
15	University hospital	1/2	34, 34	No	No
16	Regional referral hospital	3/5	32–37, 34	No	No
	Total	139/6	mean ± SD 30.2±2.6 weeks		

NA not available

possible using CT Expo software (SASCRAD, Buchholz, Germany), a program for dose evaluation in CT. However, six CTDIvol and five DLP values were treated as inappropriate data. Eventually, during a 29-month period, from October 2009 until February 2011, 119 CTDIvol and 120 DLP values from a total of 20 protocols and 125 scan data were available for this audit.

CT dosimetry

The framework for CT dosimetry has already been well established [23]. The monitoring of CT performance as part of routine quality assurance is based on the practical dose qualities of CTDIvol and DLP. These form the basis for the reference dose (and DRLs) set for the purpose of promoting the optimization of patient protection [23]. CTDIvol (units: mGy) is the mean absorbed radiation dose to the patient at a given point of scan volume expressed as a function of kVp, mAs, filtering, collimation and pitch. DLP (units: mGy cm) is an indicator of the mean absorbed dose to the patient of each series in a CT exam and is defined as the product of CTDIvol × exposed scan length [24]. To establish the DRLs, the minimum, first-quartile (25th percentile), median (50th percentile), third-quartile (75th percentile) and maximum values of CTDIvol and DLP for fetal CT were determined on the basis of all of the scan data [25]. In keeping within the established framework, the national DRLs presented in this survey were determined using the 75th percentile values of CTDIvol and DLP [15]. The median value was compared among all of the protocols (n=20) to clarify its tendency. We evaluated the interval change of CTDIvol in the hospitals presenting with three or more cases during the same period, regardless of whether dose reduction was introduced. This study was approved by the institutional review board at the National Center for Child Health and Development, Tokyo, Japan.

Results

Table 1 shows the results of epidemiological background. A total of 139 cases of fetal CT were performed throughout 6 years (range: 1–53 cases). The timing of gestational week at the CT scan ranged from 15 to 38 weeks (mean±SD: 30.2± 2.6 weeks). Only one hospital (no. 9) experienced a repeat fetal CT examination, and only hospital 4 had answered yes to use of Mioblock (MSD, Tokyo, Japan) for fetal motion control to avoid rescanning.

Table 2 shows details of 20 CT scan protocols, in which technical conditions included the specific CT scanner model, tube voltage (kVp), scan field of view, rotation time, beam width, detector configuration and pitch factor. The tube voltage was set at 100 kV in all of the cases in one hospital (hospital 8), at 100 or 120 kV in hospitals 9 and 13, and at 120 kV in all of the cases in the remaining 13 hospitals.

The range of rotation time was 0.37–0.75 s, and 75% (15/20 protocols) were carried out by 0.5 s. The beam width ranged from 10 to 40 mm (mean: 20 mm) and helical pitch ranged from 0.64 to 1.67 (mean: 1.1). For Toshiba CT scanners, variation in filters, target standard deviation, slice thickness, reconstruction function, and maximum and minimum tube current (mA) are summarized. For GE CT scanners, protocol 8c was obtained with iterative reconstruction (ASIR: Adaptive Statistical Iterative Reconstruction). The setting of automatic exposure control, quality reference mAs, and minimum and maximum effective mAs are summarized. For Siemens scanners, parameters for CARE Dose 4D are summarized. Throughout the 20 protocols, iterative reconstruction was only performed in protocol 8c, while the other 19 were carried out without it.

Table 3 shows the data of CTDIvol (median), sample number of CTDIvol, DLP (median), sample number of DLP, scan length (average) mm and interval change of CTDIvol in all of the 20 protocols. Protocol number 8c, which was only performed with iterative reconstruction, showed the lowest median CTDIvol (2.6 mGy). However, there was no other obvious relationship between technical data (number of detectors, reconstruction function and availability of 100 kV) and dose levels. Additionally, data from each scan did not correspond to patients' individual body weight or correct gestational week. Therefore, it was unknown which hospitals used higher doses of radiation to image mothers later in pregnancy. The relationship between maternal girth and weight (and by implication, gestational age), which affected CT parameters used for the examinations, was also unknown.

The scan length greatly varied between institutions (327± 47.7 cm, range: 245–440 cm, Table 3). No institution used bismuth shielding for fetal CT examinations.

Table 4 shows the minimum, first-quartile, median, third-quartile and maximum values of CTDIvol and DLP. The minimum, first-quartile, median, third-quartile and maximum values of CTDIvol were 2.1, 3.7, 7.7, 11.3 and 23.1 mGy, and the corresponding values of DLP were 69.0, 122.3, 276.8, 382.6 and 1025.6 mGy·cm, respectively. The domestic DRLs of CTDIvol and DLP for fetal CT were 11.3 mGy and 382.6 mGy·cm, respectively. The minimum, first-quartile, median, third-quartile and maximum values of scan length were 190, 295, 319, 356 and 476 mm, respectively. In Figs. 1 and 2, all 20 CTDIvol and DLP medians per protocol are plotted in ascending order, respectively. The maximum values of CTDIvol and DLP were approximately 11 and 15 times as high as their minimums, respectively. In the five protocols with a CTDIvol median of 5 mGy or less, the gap between the third- and first-quartiles tended to be smaller, and the radiation dose was similar among the cases. In contrast, the institutions with high CTDIvol medians tended to show variation in their

Table 2 Details of 20 CT protocols (technical conditions of the scan, including the hospital and protocol, specific CT scanner model, tube voltage [kVp], scan FOV, rotation time, beam width, detector configuration, pitch factor, filter, target SD, slice thickness, reconstruction function, maximum and minimum tube current [mA], ASIR, AEC, quality reference mAs, and minimum and maximum effective mAs)

Hospital / protocol	Toshiba CT scanner model	kVp	Scan FOV	Rotation time	Beam width (mm)	Detector configuration (no. of sections × mm)	Pitch factor	Filter	Parameters for volume EC				
									Target SD	Slice thickness (mm)	Reconstruction function	Minimum mA	Maximum mA
1	Aquilion 64	120	L	0.5, 0.75	32	64×0.5	0.64–0.83	None	12	5	FC13	100	350
6	Aquilion 64	120	L	0.5	32	32×1, 64×0.5	0.7–1.4	2D-Q01	10	5, 7	FC13	10	400
7	Aquilion 16	120	M	0.5	16	16×1	0.94	QDS+	9, 25	5	FC10	10	400
11	Aquilion 16	120	M	0.5	16	16×1	0.94	None	7.5	7	FC13	10	400
14	Aquilion 64	120	M, L	0.5	32	32×1, 64×0.5	0.84	QDS+	8, 15	5, 10	FC13, 15	10	450
	GE Healthcare												
	CT scanner model	kVp	Scan FOV	Rotation time	Beam width (mm)	Detector configuration (no. of sections × mm)	Helical pitch	Plus recon	ASIR	Slice thickness (mm)	Parameters for auto mA		
											AEC	Noise index	Minimum mA	Maximum mA
2	LightSpeed Ultra 16	120	L	0.6	10	16×0.625	1.37	Yes	None	5	smart mA	8.5	100	423
8 A	LightSpeed Ultra	100	L	0.5–0.7	20	8×2.5	1.67	Yes	None	5	auto mA	8 15	100	420
8 B	LightSpeed Ultra	100	L	0.5	20	8×2.5	1.67	Yes	None	5	auto mA	21	100	175
8 C	Discovery 750HD	100	L	0.4	40	64×0.625	1.37	Yes	50%	5	smart mA	21	10	175
13 A	LightSpeed VCT	100, 120	M	0.4	40	64×0.625	1.37	Yes	None	5	smart mA	7.9–15	100	770
13 B	LightSpeed Ultra 16	120	L	0.6–0.7	10, 20	16×0.625, 16×1.25	1.37	Yes	None	5	smart mA	8–8.5	100	440
	Seimens													
	CT scanner model	kVp	Rotation time	Beam width (mm)	Helical pitch	Detector configuration (no. of sections × mm)	Slice thickness (mm)	Parameters for CARE Dose 4D						
								Quality Ref. mAs	Minimum effective mAs	Maximum effective mAs				
3	SOMATOM Sensation 16	120	0.5	12	1.25	16×0.75	5 7	NA	36	47				
4 A	SOMATOM Sensation Cardiac	120	0.37	12	1	16×0.75	10	35, 70	NA	NA				
4 B	SOMATOM Definition	120	0.5	19.2	1	64×0.3	10	50–80	NA	NA				
5	SOMATOM Sensation 64	120	0.5	19.2	1.2	64×0.3	5	150	96	261				
9	SOMATOM Definition AS	100, 120	0.5	19.2	0.6	64×0.3	5	230–350	108	271				
10	SOMATOM Sensation 16	120	0.5	12, 24	0.85	16×0.75, 16×1.5	5, 8	220–280	204	500				
12	SOMATOM Sensation 16	120	0.5	12	1.15	16×0.75	5	150	56	181				

Table 2 (continued)

16	SOMATOM Sensation 16 Philips	120	0.5	12	0.9, 1.05	16×0.75	5	150	68	122				
	CT scanner model	kV	Scan FOV	Rotation time	Beam width (mm)	Detector configuration (no. of sections × mm)	Helical pitch	Slice thickness (mm)	Noise index	AEC		Minimum mA		Maximum mA
15	Brilliance iCT	120	L	0.5	80	128×0.625	0.8	5	NA	none		NA		402

FOV field of view, *SD* standard deviation, *AEC* automatic exposure control, *ASIR* Adaptive Statistical Iterative Reconstruction, NA not available

Table 3 Median CTDIvol, CTDIvol sample, median DLP, DLP sample, length and interval change of CTDIvol for 20 protocols

Hospital / protocol	CTDI vol (median) mGy	CTDIvol sample	DLP (median) mGy.cm	DLP sample	Length (ave) mm	Interval change of CTDI vol
1	12.7	7	359.8	7	357	Flat (med)
2	13.3	4	583.9	4	401	Decreased
3	3.4	5	112.2	5	272	Flat (low)
4A	2.8	3	80	5	364	Flat (low)
4B	2.9	4	89.5	4	310	
5	9.3	4	339.5	4	328.5	Increased
6	6.7	1	210	1	266	NA
7	13.6	2	280	2	245	NA
8A	7.7	33	277	33	314	Decreased
8B	3.3	11	107.8	11	314	
8C	2.6	9	101.3	9	328.3	
9	10.8	8	353	7	362	Decreased
10	11.8	4	454.5	4	318	Decreased
11	23.1	3	784	3	300	Flat (high)
12	10.1	3	403	3	440	Flat (med)
13A	10	10	372.2	10	309.5	Decreased
13B	17.7	3	887.2	3	390	
14	10.6	1	323	1	320	NA
15	13.3	1	493.6	1	280	NA
16	8.1	3	270	3	333	Flat (med)

CTDI CT dose index, *DLP* dose length product, *NA* not available, *med* medium

scanning conditions, and the gap between the third- and first quartiles tended to be greater.

Hospitals presenting with low CTDIvol values did not necessarily provide low DLP values because the length settings were different among these hospitals.

Figure 3 shows the interval changes in CTDIvol in the 12 hospitals where fetal CT was performed in three or more cases (hospitals 1–5, 8–13 and 16). Six of these 12 hospitals (hospitals 2, 5, 8, 9, 10 and 13) reduced the radiation dose during the implementation period, probably based on their own judgment. Of the remaining six hospitals, two (hospitals 3 and 4),

Table 4 Summary of the minimum, 25th, 50th, 75th and maximum CTDIvol and DLP values

	CTDI vol (mGy)	DLP (mGycm)
Minimum	2.1	69
25th	3.7	122.3
50th	7.7	276.8
75th	11.3	382.6
Maximum	23.1	1025.6

CTDI CT dose index, *DLP* dose length product

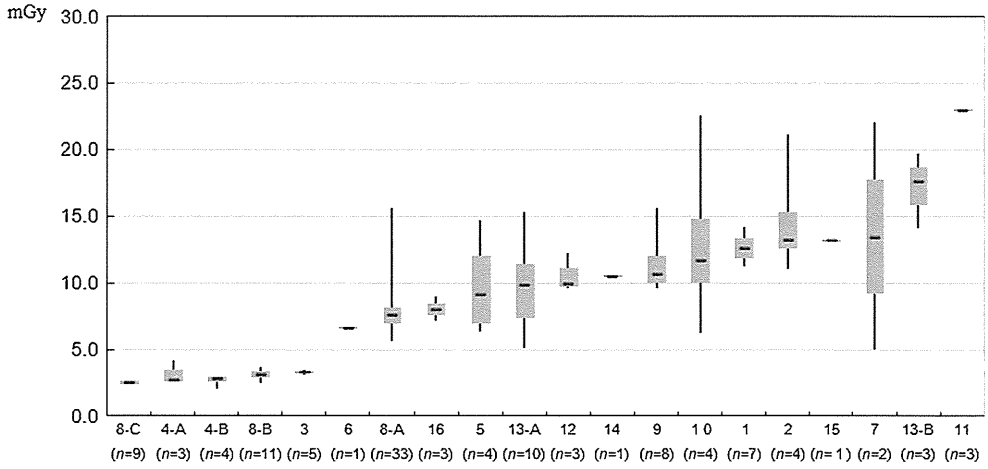

Fig. 1 Comparison of box plots of individual CTDIvol in each of the 20 protocols

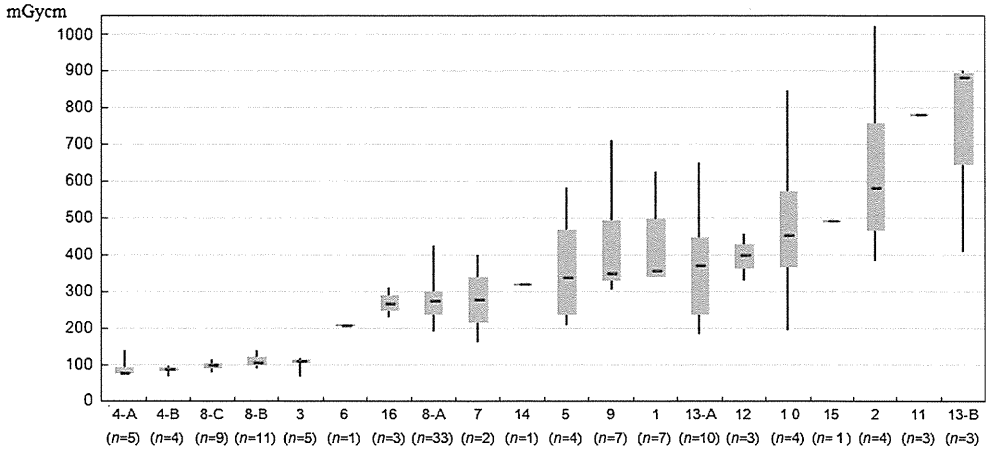

Fig. 2 Comparison of box plots of individual DLP in each of the 20 protocols

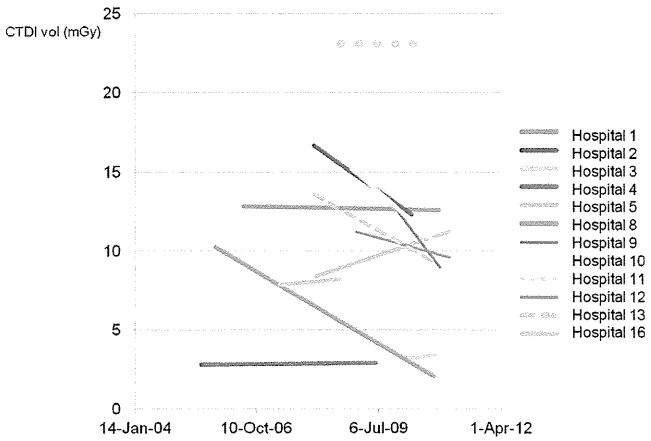

Fig. 3 Interval changes in CTDIvol in the 12 hospitals where fetal CT was performed in three or more cases (hospitals 1-5, 8-13 and 16)

three (hospitals 1, 13 and 16), and one (hospital 11) kept the radiation dose low, moderate and high, respectively.

Discussion

CT for fetal skeletal dysplasia was first reported by Shoda et al. [26] in 1997. Since then, the usefulness of this technique has been reported in case reports [27–29], a report comparing it with fetal US [3] and a review [7]. Most of these reports presented cases of monostotic, rare skeletal dysplasia or discussed diagnostic capabilities of bone morphology [6]. The weighted CT dose index of the fetal exposure dose was reported as 3.12 mGy by Cassart et al. [6], 3 mGy by Ruano et al. [3] and 1.9 mGy by Bonnefoy et al. [30]. Recently, the effective dose for low-dose fetal CT was estimated with an ImPACT CT Patient Dosimetry Calculator (CT Scanner Evaluation Center, London, UK) and reported to be 4.8 mSv by

Victoria et al. [22]. However, in their report, neither the CTDIvol nor DLP value during the scan was mentioned.

In the present study, the CTDIvol median was as low as 2.6–3.4 mGy in five protocols of three hospitals (hospitals 3, 4 and 8), and these data are similar to those in the reports mentioned above [3, 6, 30]. In these hospitals, the maximum and minimum values were stable and, therefore, radiation dose control was probably appropriately performed (Figs. 1 and 2). These values are similar to the first-quartile values calculated in this study (3.7 mGy). In these three hospitals, many images were taken at lower dose settings. At this time, a favorable, reasonable dose setting for fetal CT protocol was 3.7 mGy, which corresponds to the first-quartile value obtained in this study.

In our study, the national DRL of CTDIvol for Japanese fetal CT was estimated at 11.3 mGy. Seven hospitals (hospitals 1, 2, 7, 10, 11, 13 and 15) presented with a CTDIvol exceeding this DRL value. Of these hospitals, three (hospitals 2, 10 and 13) had a tendency to reduce the radiation dose over time. Based on our results, our study group advised these seven hospitals to reduce the radiation dose to the DRL or lower.

Concerning a time-dependent change in the exposure dose, six of the 12 hospitals reduced the dose setting during the implementation period. In particular, hospital 8 reduced the dose voluntarily by revising the protocol twice during the surveyed period. Presumably, this hospital had set a higher radiation dose at first because the setting condition was not clear. However, this hospital may have voluntarily attempted to reduce the dose while maintaining image quality. Their efforts should be appreciated in terms of the ALARA principle. Two of the other six hospitals kept the radiation dose at a moderate or high level, and they should change their protocol according to the DRL results.

Our CTDIvol and DLP values were derived from the dose radiated by the equipment and are not equivalent to the fetal exposure dose. The fetal exposure dose cannot be directly measured and must be estimated. If each hospital uses a human pelvis phantom, the fetal exposure dose can be estimated individually. A previously reported technique to estimate the fetal exposure dose was also useful [31]. The easiest method to assess the fetal exposure dose may be to simply use the uterine organ dose calculated with the commercially available Monte Carlo simulation software [22].

In our study, the fetal exposure dose was not estimated for each case. However, this dose should be much lower than the threshold of occurrence of central nervous system anomalies, which is specified in the International Commission on Radiological Protection Publication 87 (100 mGy, first trimester) [32]. In addition, it is difficult to appropriately estimate carcinogenesis due to low-dose exposure in the fetus. Hurwitz et al. [33] estimated the fetal exposure dose in pregnant women subjected to appendicitis or chest CT. They found that the fetal exposure dose was 30 mGy in pregnant women subjected to an appendicitis CT protocol, and the risk of childhood carcinogenesis from this fetal exposure dose was approximately twice as high as that for natural childhood carcinogenesis (The excess relative risk of developing childhood cancer 2:600) [33]. While the DRL of CTDIvol was estimated as approximately 11 mGy in this study, this value must be converted to the fetal exposure dose. If the fetal exposure dose is approximated at 1.3 times that of CTDIvol [34], the risk of childhood carcinogenesis from this fetal exposure dose may be less than that for the appendicitis CT protocol described above.

Recently, the risk of leukemia and brain tumors from childhood CT exposure has been reported [35], but the risk of future carcinogenesis from fetal CT exposure remains unknown. When state-of-the-art technology, such as iterative reconstruction, is widely used in CT equipment in the near future, the exposure dose for CT scans can be decreased to 1 mSv or less [36]. However, before this is achieved, each hospital should use CT doses as low as possible on the principle of ALARA.

Based on our study results, we should reduce the exposure dose voluntarily and control the exposure dose throughout Japan. Moreover, we should implement a similar study after 3 or 4 years to confirm that the radiation dose has decreased after the establishment of DRLs by the committee of the Japan Society of Obstetrics and Gynecology. Depending on the results of the next study, it may be necessary to review the DRLs and reset them at lower values.

Conclusion

The national DRLs of CTDIvol and DLP for fetal CT in Japan were estimated as 11.3 mGy and 382.6 mGy·cm, respectively. Based on these results, the exposure dose should be voluntarily reduced and the exposure dose should be controlled to continue promoting fetal CT that involves radiation exposure.

Acknowledgments This article was supported by a grant-in-aid for Scientific Research from the Ministry of Health, Labour and Welfare of Japan, H23-Nanchi-Ippan-123.

We very much appreciate the cooperation of the following subgroup members of the above research project: Dr. Yoshihisa Shimanuki, radiologist, and Mr. Kiyoaki Sasaki, chief radiological technologist, Miyagi Children's Hospital; Mr. Hiroshi Nagamatsu and Ms. Ayano Shimada, radiological technologists, National Center for Child Health and Development; and Dr. Chihiro Tani, radiologist, and Mr. Masao Kiguchi, radiological technologist, Hiroshima University. Moreover, we very much appreciate the cooperation of all obstetricians, radiologists, and radiological technologists in all 16 hospitals.

Conflict of interest None

References

1. Warman ML, Cormier-Daire V, Hall C et al (2011) Nosology and classification of genetic skeletal disorders: 2010 revision. Am J Med Genet A 155:943–948